Advanced Study Workshop on Earthquake Engineering

Soliton-Like Interaction Waves in Underground Pipelines Under Seismic Impacts

AIPCP25-CF-ASWEE2025-00025 | Article

Soliton-Like Interaction Waves in Underground Pipelines Under Seismic Impacts

Karim Sultanov[1, a)], Sabida Ismoilova[1,] and Nodirbek Akbarov[1]

[1]*Institute of Mechanics and Seismic Stability of Structures named after M.T. Urazbaev, Uzbekistan Academy of Sciences, Tashkent, Uzbekistan*

[a)] Corresponding author: sultanov.karim@mail.ru

Abstract. The paper examines non-stationary wave problems related to the longitudinal interaction between underground trunk pipelines and the surrounding soil under seismic loads. Specifically, it focuses on the propagation of a longitudinal wave along the pipeline. The problem is simplified into two coupled one-dimensional problems. The pipeline is modeled as a viscoelastic hollow semi-infinite rod. To describe the deformation of the rod, the authors utilize the Eyring model (the standard-linear body model). In certain cases, this model can be easily transformed into the elastic Hooke model. Similarly, the soil surrounding the pipeline is modeled as a semi-infinite hollow rod, where the internal diameter is equivalent to the external diameter of the pipeline. The depth at which the pipeline is buried in soil and its external radius determine the external diameter of the surrounding hollow "soil rod". The equations governing the soil's behavior are also based on the viscoelastic Eyring model. Consequently, the calculation model represents a coaxial system-a "pipe within a pipe". The seismic wave propagates exclusively through the soil, starting from a designated initial section. The wave formation along the pipeline is a result of the interaction force (friction) at the contact surface between the pipeline and soil. This frictional force acts on the pipeline's outer surface. The wave problems are addressed separately for the pipeline and soil, but they are interconnected through the conditions at their contact interface. These conditions follow nonlinear laws governing the friction force and can be divided into two stages. In the first stage, the friction force increases in proportion to the relative displacement. In the second stage, the friction behavior is described by the Amontons-Coulomb law. To obtain a numerical solution, we use the method of characteristics, followed by the finite difference method. An analysis of the numerical results shows that, under the influence of the active interaction force (friction), soliton-like waves are generated in the pipeline and propagate along the pipeline without attenuation.

INTRODUCTION

The construction of underground pipelines is globally on the rise, making them critical components of energy and construction projects [1, 2]. One of the primary challenges in this field is ensuring the strength and safe operation of these pipelines, particularly in the event of seismic activity. As noted in reference [1], even minor seismic forces can result in significant damage and accelerate failures in certain pipeline sections, especially when the pipeline runs parallel to the direction of the seismic load. The transportation of natural gas, oil, and petroleum products through pipelines underscores the importance of their seismic resistance and stability.

When discussing the seismic resilience of underground structures [3-5], the focus is often on the movement and vibrations of the pipelines themselves. However, it is essential to recognize that the stress-strain conditions of the soil surrounding the pipeline play a significant and, sometimes, decisive role in determining the overall stress state of the pipeline [6]. Key factors influencing the stress-strain state of the pipeline include soil deformation around it and the structural failure of soil during its interaction with the pipeline [7-10]. From a mechanical behavior perspective, structural failure of soil occurs when there is a change in the mechanical characteristics of soil [9, 10].

The reliability and strength of underground pipeline systems largely depend on the interaction forces resulting from the relative movement between the pipelines and the surrounding soil, as noted in reference [3]. One key aspect to consider is the stress state and dynamic behavior of the soil around the underground pipelines, as highlighted in reference [6]. Current theories on the seismic resistance of underground structures, such as those cited in references [3 to 5], do not adequately account for this factor. Additionally, many existing theories primarily focus on stationary

oscillations of pipelines without considering the influence of the soil medium, as discussed in references [3, 4]. Taking the surrounding soil medium into account when addressing non-stationary problems necessitates solving boundary wave issues.

Non-stationary boundary value problems related to the propagation of seismic waves in soils are discussed in [8]. When a pipeline is embedded in a soil medium, seismic loads and the deformation properties of soil and the pipeline create interaction forces at their contact surfaces. The longitudinal interaction laws between an underground pipeline and the surrounding soil are examined in [9]. These laws exhibit significant nonlinearity, particularly due to the destruction of the soil contact layer during strong interactions, as highlighted in [10]. In [6], the application of this interaction law to the seismic resistance of underground pipelines is demonstrated. However, solutions to wave problems in this context can only be derived using numerical methods.

Numerous studies focus on wave processes in soils and the numerical methods for solving wave problems related to soils and underground pipelines; for example, see [11-15]. In [11], an analytical solution is presented for the seismic response of a transverse wave falling on a layered elastic foundation under dynamic impact, based on the theory of wave propagation. Additionally, reference [12] proposes an integrated method for inverting dispersion curves of directed longitudinal waves and surface waves, which allows for the simultaneous estimation of longitudinal and shear wave velocities.

In [13], a theoretical investigation is conducted on the propagation of longitudinal acoustic waves in structurally inhomogeneous viscoelastic solids that exhibit some nonlinearity, which decreases with increasing frequency. The study provides exact solutions for standing waves that propagate without any change in their shape.

The examination of wave processes in soils is particularly relevant when considering wave interactions with structures within a soil environment. Among the most common and significant underground structures are trunk pipelines. In [14], the influence of dynamic behavior and lateral soil pressure on the dynamics of box culvert pipes buried in dry, loose soils is numerically investigated.

The review article [15] discusses the perfectly matched layer (PML) method and its various formulations developed over the past 25 years for numerical modeling and simulation of wave propagation in unbounded media. Additionally, a brief analysis of publications in [16], addressing the seismic interaction of soils and structures, indicates that wave processes in soils and underground pipelines are being studied intensively worldwide.

The findings in references [17 to 19] indicate that creating mathematical models for wave propagation in soils and their interaction with underground structures, along with solving numerical wave problems, is a significant and quite labor-intensive task.

MATERIALS, METHODS, AND OBJECTS OF STUDY

The general statement of the problem of wave propagation in soil containing an underground pipeline laid at a certain depth, as illustrated in Fig. 1, is inherently three-dimensional. However, mathematical modeling and finding a numerical solution for this problem can pose significant mathematical and physical challenges. To simplify the analysis, we will adopt a more straightforward model and calculation scheme. For our calculations, we will use a coaxial composite rod system consisting of two layers along the radius.

In this model, the outer hollow rod represents the soil medium, while the inner rod represents the pipeline. Since we are focusing on the trunk pipeline, we will assume it to be sufficiently long, starting from the initial section x=0. This initial section (x=0, where x is the axis of the pipeline) will be considered a fixed point where the seismic wave is set in soil.

This calculation scheme greatly simplifies the three-dimensional problem by reducing it to two one-dimensional problems. This method of simplification has been effectively utilized in references [3, 5, 6]. While this approach simplifies the problem significantly, it still captures the main characteristics and essence of the wave processes in soil and the pipeline.

The mathematical model of soil and pipeline deformation is taken to be linear-viscoelastic
(a standard linear body):

$$\frac{d\varepsilon_i}{dt} + \mu_i \varepsilon_i = \frac{d\sigma_i}{E_{Di} dt} + \mu \frac{d\sigma_i}{i E_{Si}}$$
$$\mu_i = E_{Di} E_{Si} / (E_{Di} - E_{Si}) \eta_i \quad (1)$$

Here and below, i=1.2. For i=1, the parameter values refer to the pipeline, and for i=2, to the soil.

In Eq. (1), σ– is the longitudinal stress, ε– is the longitudinal strain, t – is time, E_S– is the static modulus of elasticity, E_D – is the dynamic modulus of elasticity, μ– is the bulk viscosity parameter, η– is the bulk viscosity coefficient.

In [9], based on serial laboratory and field static and dynamic experiments on the interaction of an underground pipeline with soil, mathematical models of interaction for changing the interaction force (friction) τ were developed. The most adequate of them is the model developed based on a standard linear body in the following form: in a homogeneous, isotropic, linearly elastic body are defined as:

for $\sigma_N > \sigma_N^*$, $0 \le u \le u_*$:

$$\frac{d\tau}{K_{xD}(\sigma_N, I_S)dt} + \mu_S(\sigma_N, I_S, \dot{u})\frac{\tau}{K_{xS}(\sigma_N, I_S)} = \frac{du}{dt} + \mu_S(\sigma_N, I_S, \dot{u})u \tag{2}$$

for $\sigma_N > \sigma_N^*$, $u > u_*$:

$$\tau = c + f\sigma_N \tag{3}$$

for, $\sigma_N \le \sigma_N^*$:

$$\tau = 0 \tag{4}$$

where τ– is the interaction (friction) force, u– is the relative displacement, $u=u_g-u_c$, u_g– is the absolute soil displacement, u_c– is the absolute pipeline displacement; u_*– is the critical value of the relative displacement, upon reaching which the soil contact layer is completely destroyed; K_{xD} – is the variable dynamic soil stiffness coefficient (as $\dot{u} \to \infty$); K_{xS} – is the variable static soil stiffness coefficient (as $\dot{u} \to 0$); μ_S – is the variable parameter of soil shear viscosity; $\dot{u}=du/dt$– is the rate of relative displacement of the pipeline and soil; $I_S=u/u_*$ – is the parameter characterizing the structural destruction of the soil contact layer, $0 \le I_S \le 1$, for $I_S=0$ is the soil contact layer when contact bonds between the outer surface of the pipeline and the soil are intact, and for $I_S=1$, this bond is completely destroyed; f_v– is the coefficient of internal friction of the soil; σ_N– is the stress normal to the outer surface of the pipeline; σ_N^*– is the ultimate tensile strength of the soil (from here on, compressive stresses are taken to be positive). Specific nonlinear functions of equations (2) and physical values of the parameters included in equations (2) – (4) are given in [6, 9].

The equations for the longitudinal motion of the pipeline and soil along the x–axis, coinciding with the pipeline axis, are of the following form:

$$\begin{aligned} &\rho_{0i}\partial v_i / \partial t - \partial\sigma_i / \partial x + \chi_i\sigma_{\tau i} = 0 \\ &\partial v_i / \partial x - \partial\varepsilon_i / \partial t = 0 \end{aligned} \tag{5}$$

where v_i– is the particle velocity (mass velocity); σ_i, ε_i – are longitudinal stresses and strains; ρ_{0i}– is the initial density; $\chi_i=sign(v)$– for the rod, and $\chi_i=-sign(v)$– for soil; $v = v_2$ – is the soil particle velocity; σ_τ – is the reduced friction force acting per unit length of the rod.

The values of σ_τ for the pipeline and soil are determined from the following relationship:

$$\sigma_{\tau i} = 4D_{Hi}\tau / (D_{Hi}^2 - D_{Bi}^2) \tag{6}$$

where τ – is the friction force (shear stress), determined from equations (2)–(4); D_{Hi} – are the outer diameters, and D_{Bi} – are the inner diameters of the pipeline and soil.

The solution to the problem is reduced to integrating the nonlinear system (5), closed by equations (1), separately for the pipeline (i = 1, an internal problem) and separately for the soil (i = 2, an external problem). This system is coupled by nonlinear conditions on the contact surface between the pipeline and the soil, which determine the laws of variation of the interaction force (friction) τ according to equations (2)–(4).

Boundary conditions are at x = 0, the load is specified as a sinusoidal wave at the initial cross–section of soil (Fig. 1):

$$\begin{aligned} &\sigma = \sigma_{\max}\sin(\pi t/T), 0 \le t \le \theta \\ &\sigma = 0, t > \theta \end{aligned} \tag{7}$$

where T– is the half–period of the load, θ – is the duration of the load, σ_{max} – is the amplitude of the load, and σ – is the longitudinal stress acting along the x–axis.

The wave front conditions in soil and the pipeline are zero, and the initial conditions of the problems are also zero.

The systems of equations (1) and (5) are hyperbolic. They exhibit real characteristics and characteristic relations along the characteristic lines on the characteristic plane t, x. Further solutions can be derived using these characteristic relations, which are ordinary differential equations. The main equations (5), which are closed by equation (1), are classified as partial differential equations. The characteristic relations are described by ordinary differential equations.

Typically, numerical solutions to ordinary differential equations offer a higher order of accuracy compared to numerical solutions for partial differential equations [17].

As previously mentioned, the underground pipeline is involved in the movement of the soil medium, along which the seismic wave propagates. According to reference [17], the frequency of longitudinal seismic waves can vary between 0.01 and 100 s^{-1}. Reference [8] indicates that high-frequency seismic waves in soils attenuate significantly and do not carry substantial energy. Conversely, low-frequency seismic waves, which contain the primary energy of an earthquake, are considered the most dangerous.

Based on these assumptions, we have chosen initial data for calculations using the developed computer program. Research conducted in [17] indicates that during strong earthquakes, the amplitude of longitudinal waves can reach σ_{max}= 0.3-0.7 MPa.

To conduct numerical calculations, we selected characteristics for loess-like soils, commonly found in seismically hazardous regions of the Earth.

Consequently, we will use the following parameter values as the initial inputs for our numerical calculations.

Soil characteristics are: γ_{0g}= 20 kN/m^3 – specific gravity of soil; D_{Ng}= 3 m – nominal external diameter of the soil cylinder; D_{Bg} = 0.15 m – nominal internal diameter of the soil cylinder; K_σ= 0.3 – soil lateral pressure coefficient; γ_g=γ_2=E_{Dg} / E_{Sg}=2– dimensionless quantity; C_{0g}= 1000 m/s – longitudinal wave propagation velocity in soil; C_{gS} = 500 m/s – transverse wave propagation velocity in soil.

Characteristics of steel pipelines are: γ_{0c} = 78 kN/m^3 – specific gravity of the pipeline material; D_{Nc} = 0.15 m – outer diameter of the pipeline; D_{Bc} = 0.14 m – inner diameter of the pipeline; γ_c=γ_1=E_{Dc} / E_{Sc}=1.02– dimensionless quantity; C_{0c} =5000 m/s – velocity of longitudinal waves in pipeline; H_1=1.425 m – depth of pipeline in soil; μ_c=10000 s^{-1} – viscosity parameter of steel; L_c =107 m – nominal length of pipeline.

Characteristics of soil contact layer and soil-pipeline interaction: f_v=0.3 – coefficient of internal friction of soil; C_v =10 kN/m^2 – coefficient of soil cohesion; u_*=10–3 m – value of relative displacement at which the interaction process passes to the stage of Coulomb friction; α=1.5 – dimensionless coefficient in formula; χ=0.1 – dimensionless exponent in formula; γ_{vN}=K_{xDN} / K_{xSN}=2– dimensionless quantity; γ_{v*}=K^*_{xD}/K^*_{xS} =4– dimensionless quantity.

Load characteristics are: σ_{max}=0.7 MPa – longitudinal wave amplitude; T= 10 s – half–period of low–frequency longitudinal wave; θ= 100 s – conventional time of action of longitudinal wave; f= 1/2 T =0.05 s–1 – frequency of longitudinal wave in soil.

With the initial data given above, the frequency of longitudinal seismic waves is f = 1/2 =0.05 s^{-1}. This is a fairly low-frequency wave. However, implementation on a computer and obtaining a numerical solution encounter the most difficulties and peculiarities with low-frequency seismic waves.

However, obtaining a numerical solution and implementing it on a computer presents significant challenges, particularly with low-frequency seismic waves.

The above initial data are basic. In cases of their change in the future, it should be noted separately.

ANALYSIS OF RESULTS

Obtaining numerical solutions of nonlinear wave problems for soil media, as shown in [6, 9, 17], is a complex process, even in the case when these problems are one-dimensional in space. In cases where coupled one-dimensional issues are considered (i.e., an underground pipeline in soil), these difficulties increase significantly.

Changes in longitudinal stresses in pipeline sections x= 0; 5; 10; 15; 20; 25 and 30 m are shown in Fig. 1, curves 1-7, respectively.

Longitudinal stresses in the pipeline reach a maximum of σ_{cmax} = 148.2 MPa. This value exceeds the amplitude of the longitudinal stress in soil, which is σ_{gmax} = 0.35 MPa by a factor of 423.4. Such a significant increase is due to the active friction force that arises from soil deformation in the longitudinal direction (along the pipeline axis), which acts on the underground pipeline. This maximum stress along the pipeline is achieved gradually. In the initial section of the pipeline, no load is applied, resulting in zero stress values (indicated by straight line 1). In the subsequent sections of the pipeline, x =5 m and 10 m (curves 2 and 3), the stress amplitude gradually increases. At x =15 m, it nearly reaches a maximum of 148.2 MPa (curve 4). Beyond that point, in sections of the pipeline x =20 m, 25 m and 30 m, the stress amplitude remains constant at σ_{cmax} = 148.2 MPa. Consequently, a powerful wave with this amplitude propagates along the pipeline. Calculations indicate that the propagation velocity of this wave is significantly lower than the speed of sound in the pipeline. This observation suggests the presence of a new soliton-like interaction wave, which travels at a different velocity compared to a conventional longitudinal wave in a pipeline that is not surrounded by soil medium. The investigation of this wave's properties falls outside the scope of this work and will be the focus of future research.

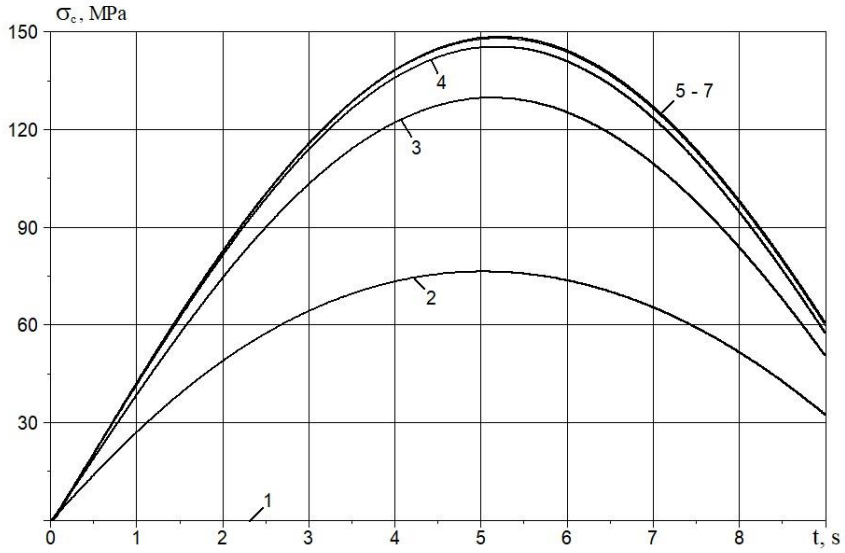

FIGURE 1. Changes in longitudinal stresses over time in the pipeline sections x = 5; 10; 15; 20; 25 and 30 m (curves 1-7).

Figure 2 illustrates the changes over time in longitudinal deformation of soil (represented by curves 1^0-7^0) and the pipeline (curves 1-7) at x = 0; 5; 10; 15; 20; 25 and 30 m, respectively.

As shown in Fig. 2, longitudinal deformations (like stresses) in all sections of soil are the same (curves 1^0-7^0). In the pipeline, they gradually increase and approach their asymptotic values, and then remain unchanged. The maximum amplitude of longitudinal deformation in the pipeline is more than double that of the deformation in soil.

The quasi-static theory of seismic resistance for underground pipelines is based on the assumption that the deformations of soil and the pipeline are equal during seismic events. However, as illustrated in Fig. 2, this assumption is not accurate. Despite this discrepancy, the quasi-static theory continues to serve as the foundation for standard regulatory methods.

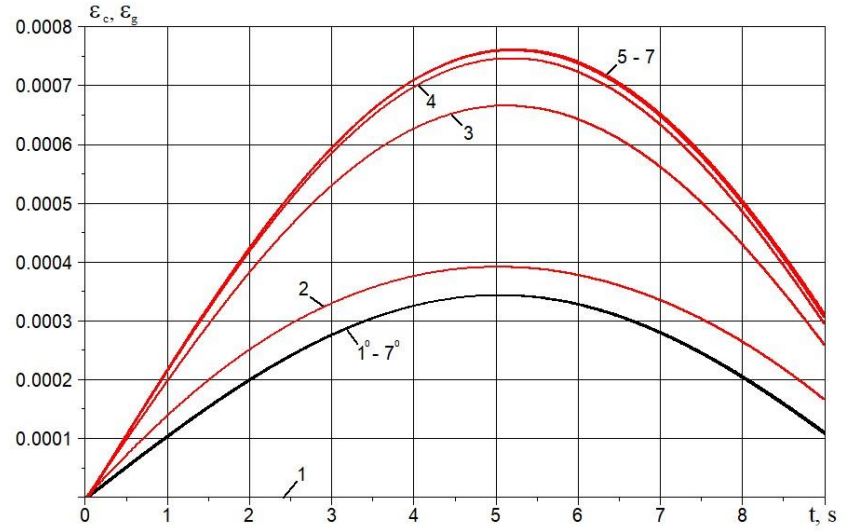

FIGURE 2. Changes in soil deformation (curves 1^0-7^0) and the pipeline (curves 1-7) over time in sections x= 0; 5; 10; 15; 20; 25 and 30 m

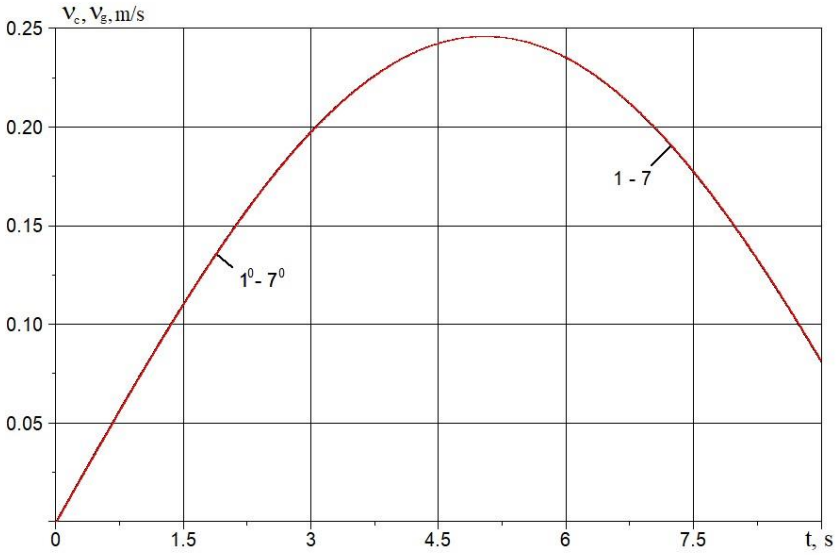

FIGURE 3. Changes in the velocity of soil particles (curves 1^0–7^0) and the pipeline (curves 1–7) over time in sections x= 0; 5; 10; 15; 20; 25 and 30 m

Figure 3 shows the changes in the velocity of soil particles (curves 1^0–7^0) and pipeline sections (curves 1–7) over time for x= 0; 5; 10; 15; 20; 25 and 30 m. As seen from Figure 3, the velocities of soil particles and pipeline sections almost completely coincide. According to the changes in the relative velocity of soil and pipeline v_t (Figure 4) for x = 0, the maximum value of the relative velocity is $0.21 \cdot 10^{-2}$ m/s (curve 1) or 0.0021 m/s. For x= 5 m - v_{tmax} = 0.0004 m/s (curve 2), and for x = 10 m - v_{tmax} = 0.0002 m/s. In the remaining sections x = 15; 20; 25 and 30 m (curves 4–7), the relative velocity values are practically zero.

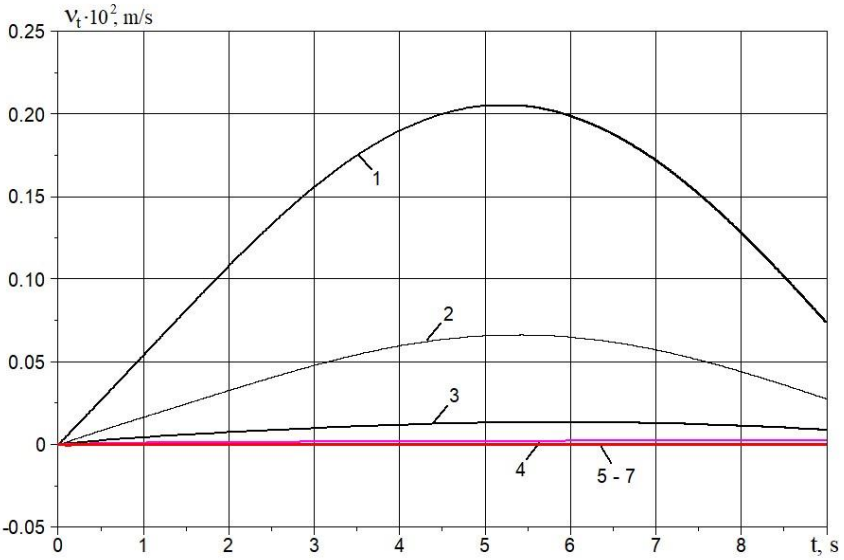

FIGURE 4. Changes in relative velocity over time in pipeline sections x= 0; 5; 10; 15; 20; 25 and 30 m (curves 1–7)

These results confirm that the velocities of soil and the pipeline ultimately become the same. According to the obtained exact analytical solutions for elastic interacting rods enclosed one inside the other, the values of the relative velocity are zero [18].

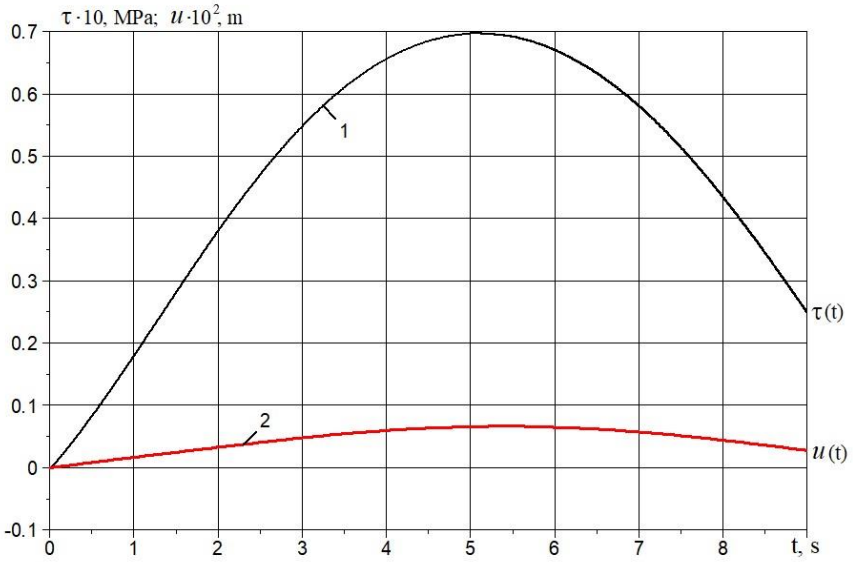

FIGURE 5. Changes in friction force (curve 1) and relative displacement (curve 2) over time for x= 5 m

Figure 5 shows the changes in the interaction force (friction) over time – $\tau(t)$ (curve 1) and the relative displacement over time - $u(t)$ (curve 2) for pipeline section x= 5 m. Similar dependencies $\tau(t)$ (curve 1) and $u(t)$ (curve 2) for x= 30 m are shown in Fig. 6. Here, the values of the shear stress (friction force) and relative displacement are quite insignificant.

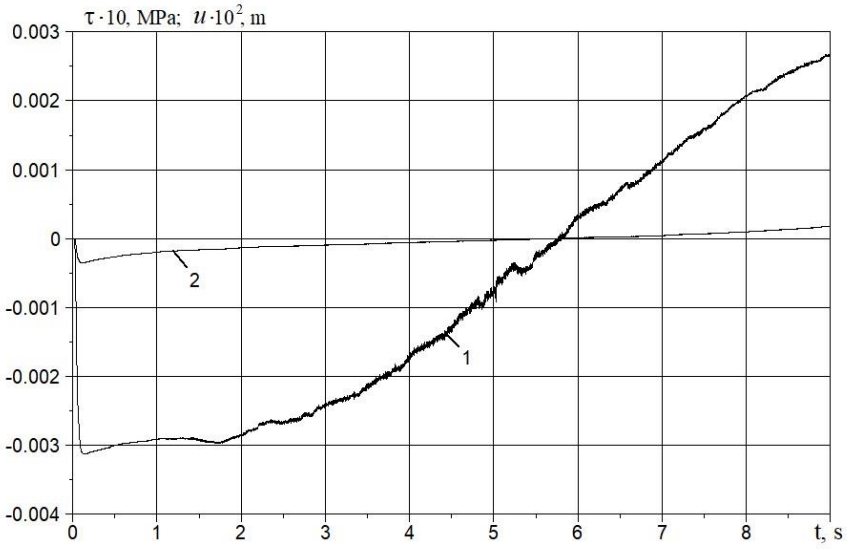

FIGURE 6. Changes in friction force (curve 1) and relative displacement (curve 2) over time for x= 30 m.

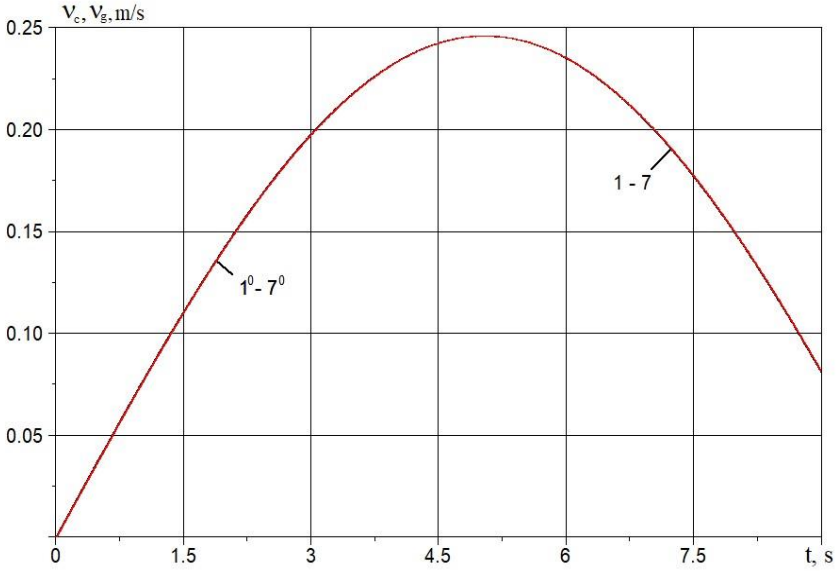

FIGURE 7. Diagrams *τ(u)* for *x*= 0, 5, and 10 m (curves 1–3)

The diagrams of the interaction of the pipeline with surrounding soil, i.e., dependencies *τ(u)*, are shown in Fig. 7 (for pipeline sections *x* = 0, 5, 10 m) and in Fig. 8 (for sections *x* = 15, 20, 25 and 30 m). From these results, it is evident that τ_{max} =0.06 MPa (curve 1 in Fig. 7) and u_{max} =0.0021 m (curve 1 in Fig. 7). Further, along the pipeline, these values of maximum interaction forces and relative displacement become even smaller. For *x*=30 m, τ_{max} =0.0002 MPa, and u_{max} =0.000025 m. In other words, the friction (interaction) force is practically absent at *x*=20, 25 and 30 m (curves 2, 3, 4 in Fig. 8). This is explained by practically identical, equal velocities of soil particles and pipeline sections, starting from sections *x*=20 m and further.

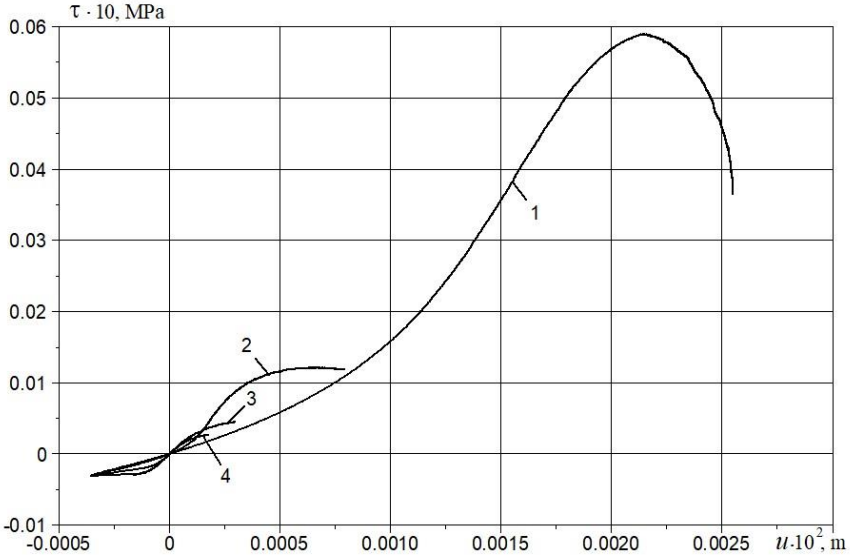

FIGURE 8. Diagrams *τ(u)* for *x*=15, 20, 25 and 30 m (curves 1–4).

CONCLUSIONS

The three-dimensional problem of underground pipeline interaction with surrounding soil during seismic wave impact can be simplified into two coupled one-dimensional non-stationary nonlinear wave problems. The calculation methods used are clearly defined and justified.

Analysis of the numerical solutions revealed that a combined nonlinear elastic-viscous-plastic interaction law and the Amontons-Coulomb law govern the interaction between underground pipelines and soil.

For the first time, it was shown that an active interaction force within an underground pipeline generates a soliton-like wave. This wave propagates along the pipeline without attenuation at a speed lower than the speed of sound in the pipeline material.

ACKNOWLEDGMENTS

The work was conducted at the expense of the grant No. AL-8924073446 of the Agency for Innovative Development under the Ministry of Higher Education, Science, and Innovation of the Republic of Uzbekistan.

REFERENCES

1. L. Muravyeva, and N. Vatin, Appl. Mech. Mater. **633–634**, 958–964 (2014). https://doi.org/10.4028/www.scientific.net/AMM.633-634.958
2. L. Muravyeva, and N. Vatin, Appl. Mech. Mater. **635–637**, 434–438 (2014). https://doi.org/10.4028/www.scientific.net/AMM.635-637.434
3. M.J. O'Rourke and X. Liu, *Response of Buried Pipelines Subject to Earthquake Effects* (MCEER, Univ. at Buffalo, USA, 1999), pp. 149-166
4. T.D. O'Rourke, J.K. Jung, and C. Argyrou, Soil Dyn. Earthq. Eng. **91**, 272–283 (2016). http://dx.doi.org/10.1016/j.soildyn.2016.09.008
5. M.S. Israilov, Mech. Solids **58**, 33-46 (2023). http://dx.doi.org/10.31857/S0572329922060083
6. K.S. Sultanov, Facta Univ., Ser. Mech. Eng. **22**, 485-501 (2024). https://doi.org/10.22190/FUME231227017S
7. K.S. Sultanov, J. Appl. Math. Mech. **62**, 465-472 (1998). https://doi.org/10.1016/S0021-8928(98)00058-6
8. K.S. Sultanov, J. Appl. Math. Mech. **66**, 115-122 (2002). https://doi.org/10.1016/S0021-8928(02)00015-1
9. K.S. Sultanov, Int. Appl. Mech. **29**, 217–223 (1993). http://dx.doi.org/10.1007/BF00847001
10. A.A. Bakhodirov, S.I. Ismailova, and K. S. Sultanov, J. Appl. Math. Mech. **79**, 587-595 (2015). https://doi.org/10.1016/j.jappmathmech.2016.04.005
11. Y. Yang and Q. Ma, J. Vib. Eng. Technol. **12**, 7441–7458 (2024). https://doi.org/10.1007/s42417-024-01306-2
12. Z. Wang, C. Sun, and D. Wu, Surv. Geophys. **45**, 429–458 (2024). https://doi.org/10.1007/s10712-023-09814-8
13. V.E. Nazarov and S.B. Kiyashko, Radiophys. Quantum Electron. **66**, 248–259 (2023). https://doi.org/10.1007/s11141-024-10291-1
14. O.L. Ertugrul, KSCE J. Civ. Eng. **20**, 1737-1746 (2016). https://doi.org/10.1007/s12205-015-0235-1
15. F. Pled and C. Desceliers, Arch. Comput. Methods Eng. **29**, 471–518 (2022). http://dx.doi.org/10.48550/arXiv.2104.09854
16. V. Anand and S.R. Satish Kumar, Structures **16**, 317-326 (2018). https://doi.org/10.1016/j.istruc.2018.10.009
17. K. S. Sultanov and N. I. Vatin, Appl. Sci. **11**, 1797 (2021). https://doi.org/10.3390/app11041797
18. L. V. Nikitin, *Statics and Dynamics of Rigid Bodies with External Friction* (Moscow, 1998), pp. 152-195 (in Russian)
19. N. E. Hoskin, Methods in Computational Physics, **3**, 265–293 (1964).